

Input referred low-frequency noise analysis for single-layer graphene FETs

Nikolaos Mavredakis and David Jiménez

Abstract—The bias-dependence of input referred low-frequency noise (LFN), S_{VG} , is a considerable facet for RF circuit design. S_{VG} was considered constant in silicon transistors but this was contradicted by recent experimental and theoretical studies. In this brief, the behaviour of S_{VG} is investigated for single-layer graphene transistors based on a recently established physics-based complete compact LFN model. A minimum of S_{VG} is recorded at the bias point where maximum transconductance is located which coincides with the peak of the well-known M-shape of the normalized output LFN and the model precisely captures this trend. Mobility fluctuation effect increases S_{VG} towards to lower currents near charge neutrality point (CNP) while carrier number fluctuation and series resistance effects mostly contribute away from CNP; thus, S_{VG} obtains a parabolic shape vs. gate voltage similarly to CMOS devices.

Index Terms—circuit design, compact model, graphene transistor (GFET), input referred low-frequency noise

I. INTRODUCTION

INPUT referred (or gate voltage) low-frequency noise (LFN) S_{VG} is a crucial figure of merit (FoM) since it can provide advantageous information regarding the selection of the operating point of analog/RF circuits. It can be defined as [1]:

$$S_{VG} = \frac{S_{ID}^2}{g_m^2} \quad (1)$$

where S_{ID} is the output or drain current LFN and g_m is the transconductance of the device. Equation (1) has been proven to be valid in all regions of operation [2]. LFN model proposed in [2] is based on carrier number fluctuation (ΔN) effect which is generated by trapping/detrapping mechanism of active traps near the gate oxide of the device [3] and assume a $(g_m/I_D)^2$ bias-dependence of normalized output noise divided by squared drain current (S_{ID}/I_D^2) where I_D is the drain current of the transistor. Such approximation which is valid under the consideration of a uniform channel at low drain voltage V_{DS} region, results in a constant S_{VG} vs. gate voltage V_{GS} (or I_D) because of (1), as shown in the following expression:

$$S_{VG} = \frac{S_{ID}^2}{g_m^2} = \frac{S_{ID}^2}{I_D^2} \frac{I_D^2}{g_m^2} = S_{VFB} \frac{g_m^2}{I_D^2} \frac{I_D^2}{g_m^2} = S_{VFB} \quad (2)$$

where S_{VFB} is the flat-band voltage spectral density related to trapped charge density [2] and is a constant.

Two more mechanisms generate LFN to semiconductor devices; mobility fluctuation ($\Delta\mu$) effect due to fluctuations of the bulk mobility which is described by the empirical Hooge

formula [4] and contact resistance contribution (ΔR) [5]. Recent experimental findings from MOSFETs prove that the approximation of a constant S_{VG} does not hold [5], [6]. An increasing trend of S_{VG} is reported towards deeper weak inversion due to $\Delta\mu$ mechanism as well as a similar increase towards stronger inversion due to ΔN and ΔR effects which result in a minimum in moderate inversion. This can be a reliable indicator for circuit designers to select the specific regime to bias the circuits. As mentioned before, the simplified $(g_m/I_D)^2$ ΔN approach predicts a constant S_{VG} , thus the aforementioned increase due to ΔN effect in higher current regime of MOSFETs is attributed to Coulomb Scattering (CS) effect [2]. The same occurs for more complete ΔN models [5, §6.3.1], where the vast percentage of this increase is still induced by CS effect.

Nowadays, new material candidates are explored to replace silicon for integrated circuits (ICs) due to the limitations on gate length scaling in CMOS devices. Among them, graphene has been proven to be an ideal contestant for RF applications due to its remarkable characteristics [7]. Graphene transistors (GFETs) have been already fabricated and used in circuits at research labs [8] but for large scale integration production, LFN and more specifically S_{VG} should be thoroughly investigated and this is the main goal of the present study. LFN is up-converted to phase noise and consequently, deteriorates the performance of analog/RF circuits such as oscillators [9] or terahertz detectors [10]. Several GFET LFN characterization and modeling studies have been reported [11]-[15] where simple S_{ID}/I_D^2 models [11], [12] based on ΔN $(g_m/I_D)^2$ approximation [2] have been proposed, whereas a complete physics-based compact model including all the LFN generators (ΔN , $\Delta\mu$, ΔR) was developed by our group [14], [15] based on a chemical-potential IV model [16]. Our model is proven to be valid in all regions of operation as it includes the effect of non-homogeneous channel on LFN as well as the contribution of Velocity Saturation (VS) effect at high electric field regime. To our knowledge, no study has been reported yet regarding the behavior of S_{VG} in GFETs. A constant S_{input} is defined in [11] which is equivalent to S_{VFB} mentioned before, but any possible bias-dependence of S_{VG} has not been explored so far. In this work, we give insight into the performance of S_{VG} at different operating conditions by validating our model with experimental data from three fabricated short-channel GFETs [17].

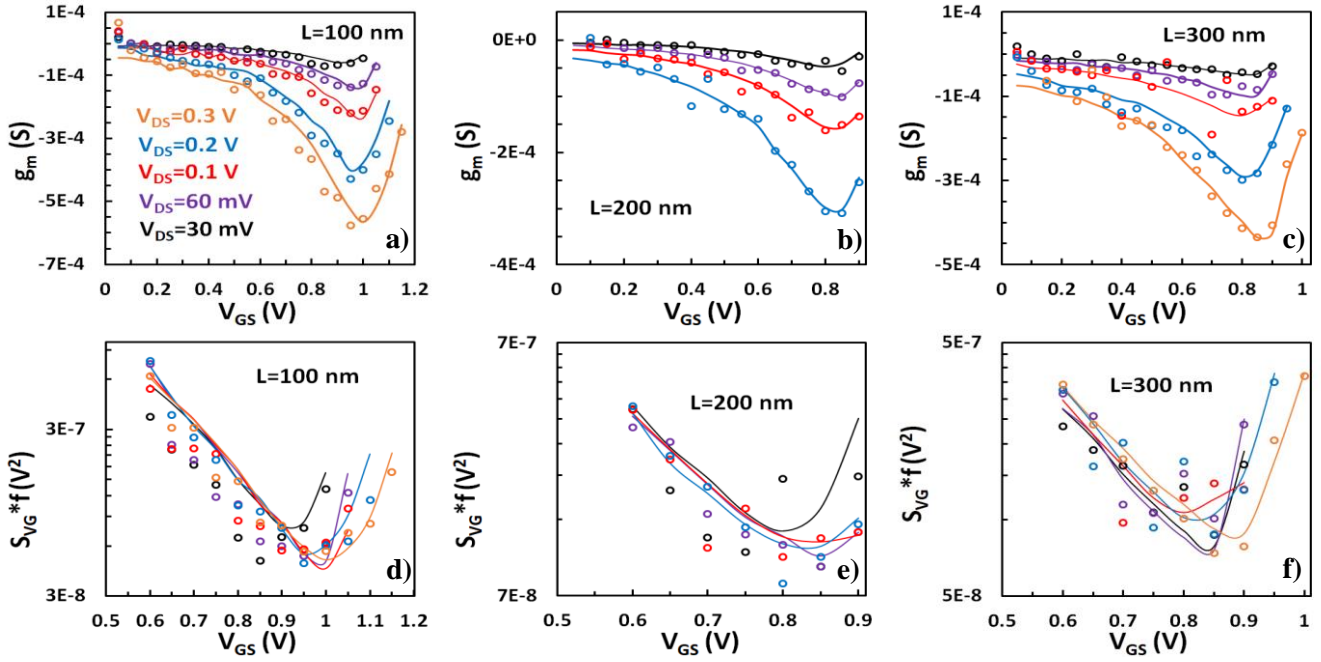


Fig.1. Transconductance g_m (upper plots) and input noise $S_{VG} * f = S_{ID} * f / g_m^2$, referred to 1 Hz, (bottom plots) vs. gate voltage V_{GS} with markers representing the measurements and lines the model for short-channel GFETs with $W=12 \mu\text{m}$ and $L=100 \text{ nm}$ (a, d), $L=200 \text{ nm}$ (b, e) and $L=300 \text{ nm}$ (c, f), respectively for all available drain voltage V_{DS} values.

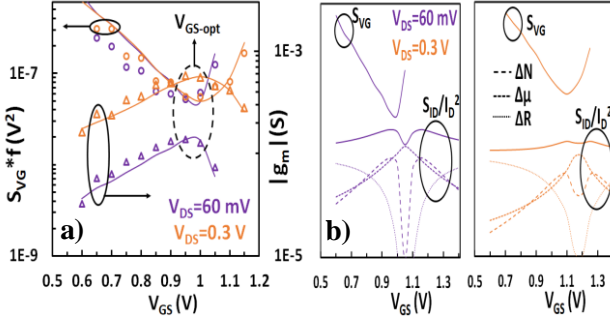


Fig.2. a) $S_{VG} * f$ (left y axis) and absolute $|g_m|$ (right y axis), b) $S_{VG} * f$, $S_{ID} * f / I_D^2$ (left y axis) vs. V_{GS} for short-channel GFETs with $W=12 \mu\text{m}$ and $L=100 \text{ nm}$ for $V_{DS}=60 \text{ mV}$, 0.3 V . markers: measured, solid lines: total model, dashed and dotted lines: different noise contributors ΔN , $\Delta \mu$ and ΔR respectively.

II. DEVICES AND MEASUREMENTS

I_D and LFN measurements were conducted at three short-channel single-layer (SL) GFETs with width $W=12 \mu\text{m}$ and gate length $L=300 \text{ nm}$ (A300), $L=200 \text{ nm}$ (A200) and $L=100 \text{ nm}$ (A100), respectively [14], [17]. The data were obtained after sweeping V_{GS} from strong p-type to strong n-type region including charge neutrality point (CNP) for a wide range of V_{DS} values, covering from low to high electric field regime. In the present work, p-type region is exclusively shown as maximum g_m is reported there [14] while asymmetries are recorded in IV data between p- and n-type region [14] due to different electron and hole mobilities or due to effects caused by parasitic junctions at graphene metal contacts (For more details on the device fabrication process and schematics as well as the measurement setup, see [14], [17]). Regarding LFN, S_{ID} was measured from 1.5 Hz to 2.5 KHz, averaged from 10-40 Hz in order to calculate its value at 1 Hz and then S_{VG} data were estimated through (1) where g_m is extracted as the first derivative of I_D w.r.t. V_{GS} .

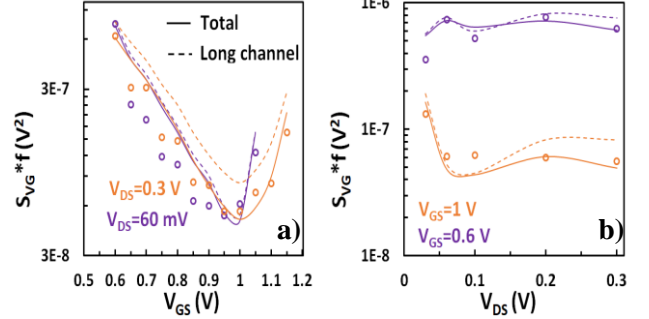


Fig.3. $S_{VG} * f$ vs. a) V_{GS} for $V_{DS}=60 \text{ mV}$, 0.3 V and b) V_{DS} for $V_{GS}=0.6 \text{ V}$, 1 V for short-channel GFETs with $W=12 \mu\text{m}$ and $L=100 \text{ nm}$. markers: measured, solid lines: total model, dashed lines: long-channel model.

In order to calculate the simulated S_{VG} through the S_{ID} model [14], [15], the value of the modeled g_m is needed in order to apply (1). Thus, it is crucial to have a precise fitting between measured and simulated g_m and this is achieved successfully as it is illustrated in Fig. 1a (A100), 1b (A200) and 1c (A300), respectively where g_m is plotted vs. V_{GS} at all available V_{DS} values. One parameter set is used for the IV simulations which can be found elsewhere [14].

III. RESULTS – DISCUSSION

A complete bias-dependent analysis of experimental S_{VG} data at $f=1 \text{ Hz}$ is presented in this section while the model is validated successfully at every operation regime. Measured S_{VG} presents a minimum versus V_{GS} for every device under test (DUT) at each individual V_{DS} from low to high electric field resulting in a parabolic shape and the model precisely captures this trend (cf. Fig. 1d-1f). (extracted LFN model parameters can be found elsewhere [14].) It is also evident that the magnitude of this minimum S_{VG} has a slight V_{DS} dependence while the whole S_{VG} shifts slightly to higher V_{GS}

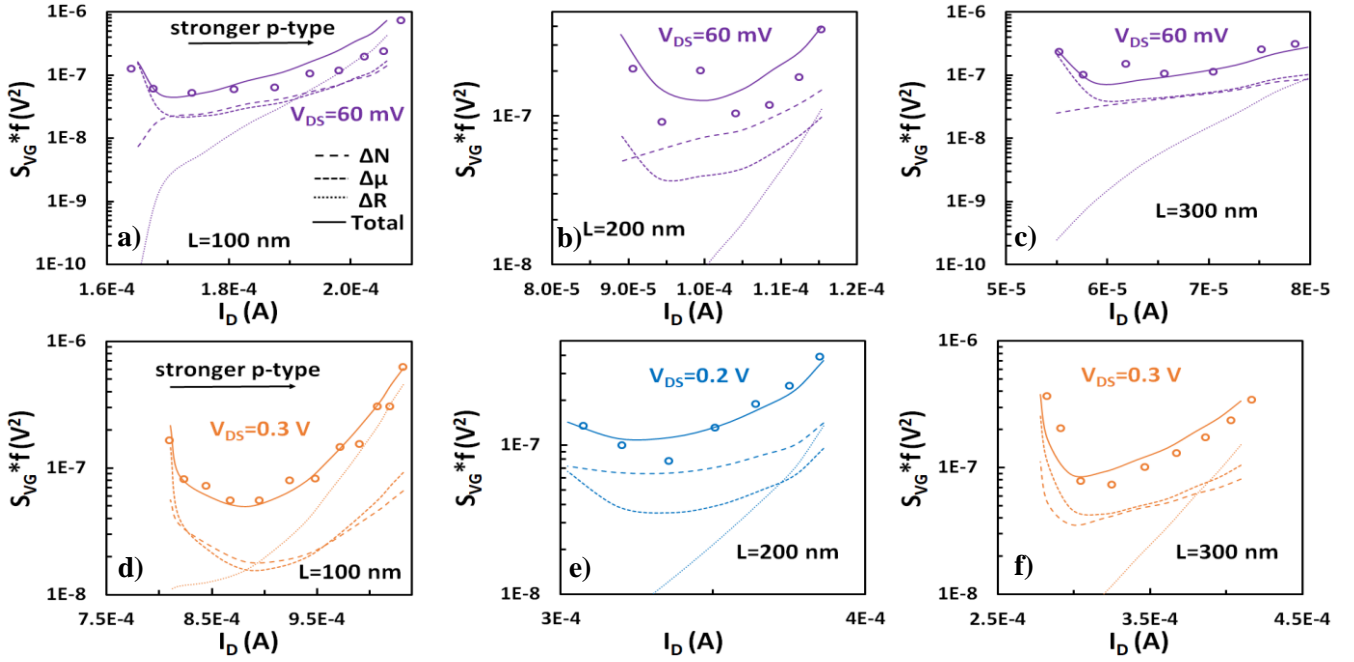


Fig. 4. $S_{VG} * f$ vs. drain current I_D for short-channel GFETs with $W=12 \mu\text{m}$ and $L=100 \text{ nm}$ (a, d), $L=200 \text{ nm}$ (b, e) and $L=300 \text{ nm}$ (c, f), respectively for low $V_{DS}=60 \text{ mV}$ (upper plots) and higher $V_{DS}=0.2, 0.3 \text{ V}$ (bottom plots). markers: measured, solid lines: total model, dashed and dotted lines: different noise contributors ΔN , $\Delta\mu$ and ΔR respectively.

as V_{DS} increases which can be justified by the corresponding increment of V_{CNP} [14]-[16]. In general, S_{VG} is nearly independent of V_{DS} towards p-type region below the V_{GS} value where its minimum is recorded ($V_{GS} < V_{GS-MINSVG}$), and the model captures this trend. Looking thoroughly to the $V_{GS-MINSVG}$, one could notice that it is located in the same point where maximum $|g_m|$ is achieved ($V_{GS-MAXGM} = V_{GS-MINSVG} = V_{GS-opt}$) for all DUTs and this can be explained by (1) where g_m is in the denominator. The latter is shown in Fig. 2a vs. V_{GS} for the A100 GFET both low $V_{DS}=60 \text{ mV}$ and high $V_{DS}=0.3 \text{ V}$. S_{VG} is shown in the left y-axis while $|g_m|$ in the right. Up to now, S_{ID}/I_D^2 was shown to be maximum at the same preceding point where the peak of the well-known ΔN effect related M-shape is also reported [11]-[15] and this is confirmed by our simulations in Fig. 2b (left subplot: $V_{DS}=60 \text{ mV}$, right subplot: $V_{DS}=0.3 \text{ V}$, $S_{VG}-S_{ID}/I_D^2$: left y axis) vs. V_{GS} where ΔN , $\Delta\mu$, ΔR effects are also presented. The latter indicates that V_{GS-opt} ensures minimum S_{VG} appropriate for biasing circuits in terms of LFN performance despite the maximum S_{ID}/I_D^2 recorded there.

In Fig. 3 both measured and modeled S_{VG} are presented vs. V_{GS} (Fig.3a) and V_{DS} (Fig.3b) for the A100 DUT whereas a long-channel model after de-activating VS effect [14], [15] is also depicted with dashed lines. Both low and high $V_{DS}=60 \text{ mV}$, 0.3 V cases are drawn in Fig. 3a and a decrease of the total model (similarly to S_{ID}/I_D^2 [14], [15]) is observed at high V_{DS} which is accurately confirmed by the experimental data. This reduction is associated with VS effect which has been successfully incorporated in our model [14], [15]. Oppositely, the long-channel model overestimates noise in the high V_{DS} case while it coincides with the total model at low V_{DS} where VS effect is insignificant. Regarding Fig. 3b, S_{VG} is illustrated for two V_{GS} values; near ($V_{GS}=1 \text{ V}$) and away ($V_{GS}=0.6 \text{ V}$) CNP. At higher V_{DS} , the complete model

predicts successfully experimental S_{VG} while the long-channel one overestimates it and the latter is more evident near CNP ($V_{GS}=1 \text{ V}$). No strong deviations are observed to S_{VG} with respect to V_{DS} away from CNP confirming its independence of V_{DS} while near CNP there is a steep decrease of S_{VG} from $V_{DS}=30 \text{ mV}$ to 60 mV while it slightly changes for the rest of higher V_{DS} values. This decrease is attributed to $V_{GS}=1 \text{ V}$ being higher than V_{GS-opt} at $V_{DS}=30 \text{ mV}$ and thus S_{VG} has already started to increase in contrary with the rest of V_{DS} cases which exhibit higher V_{CNP} and consequently higher V_{GS-opt} (cf. Fig. 1d).

In order to investigate deeper the contribution of each of ΔN , $\Delta\mu$ and ΔR mechanisms to S_{VG} , an explicit analysis is demonstrated in Fig. 4 where S_{VG} is sketched vs. I_D for low (cf. Fig. 4a-4c) and high (cd. Fig. 4d-4f) V_{DS} for all the available GFETs. Apart from the measurements and the total model, each individual contribution is shown with dashed and dotted lines for every case. It is evident that ΔN effect increases S_{VG} with I_D away from CNP towards p-type region below V_{GS-opt} for both low and high V_{DS} . It is worth mentioning that this increase is recorded without the impact of CS effect as in MOSFETs since the LFN model fits the data without the contribution of the aforementioned mechanism. Near CNP above V_{GS-opt} , ΔN contribution decreases as I_D is lessened for low V_{DS} which is reasonable as S_{ID}/I_D^2 is quite imperceptible there (deep minimum of M-shape, cf. Fig. 2b [14], [15]). In the contrary, at high V_{DS} , ΔN has a sizeable effect on S_{VG} near CNP and adds to its increase with $1/I_D$ noticed there as the non-homogeneous channel results in an increase of the minimum of S_{ID}/I_D^2 M-shape, cf. Fig. 2b [14], [15] which apparently affects S_{VG} also. ΔN contribution continues to grow with I_D , at stronger p-type region both at low and high electric fields where with the simultaneous effect of ΔR effect, a further and steeper boost

is caused to S_{VG} especially at high V_{DS} region; ΔR is trivial near CNP. Regarding $\Delta\mu$ effect, it is mainly responsible for the increase of S_{VG} with $1/I_D$ near CNP above V_{GS-opt} . $\Delta\mu$ main contribution to S_{ID}/I_D^2 has been shown to be near CNP [14], [15] (cf. Fig. 2b), and this is confirmed regarding S_{VG} in the present study. $\Delta\mu$ effect is also noticed to increase with I_D towards stronger p-type region below V_{GS-opt} at both high and low V_{DS} and thus, can moderately contribute to S_{VG} even away CNP. The above theoretical observations are successfully verified on experimental data from all the DUTs (cf. Fig. 4.)

IV. CONCLUSIONS

Input referred LFN is for the first time analyzed thoroughly for SL GFETs in this brief. The assumption of a constant S_{VG} versus V_{GS} is experimentally proven to be incorrect in GFETs, similarly to CMOS. Instead, a parabolic-like behavior is demonstrated around an optimum V_{GS-opt} point where $|g_m|$ is maximized. The coexistence of maximum $|g_m|$ and minimum input LFN can certainly induce an attractiveness from the circuit design aspect regarding the specific point. We successfully validated our recently proposed LFN model with the above experimental findings where $\Delta\mu$ mechanism is proven to mainly increase S_{VG} as I_D is reduced near CNP above V_{GS-opt} whereas below this, ΔN leads to an S_{VG} increment towards stronger p-type region which becomes even steeper with the concurrent contribution of ΔR effect far away from CNP.

ACKNOWLEDGEMENTS

We acknowledge Prof. Henri Happy, Associate Prof. Emiliano Pallecchi and Dr. Wei Wei from Carbon group (IEMN institute, University of Lille, France) for fabricating the GFET under test. This work was funded by the European Union's Horizon 2020 research and innovation program under Grant Agreement No. GrapheneCore2 785219 and No. GrapheneCore3 881603. It has also received partial funding from the Spanish Government under the project RTI2018-097876-B-C21 (MCIU/AEI/FEDER, UE); and partial funding from the ERDF allocated to the Programa Operatiu FEDER de Catalunya 2014-2020, with the support of the Secretaria d'Universitats i Recerca of the Departament d'Empresa i Coneixement of the Generalitat de Catalunya for emerging technology clusters to carry out valorization and transfer of research results. Reference of the GraphCAT project: 001-P-001702.

REFERENCES

- [1] S. Christensson, I. Lundstrom and C. Svensson, "Low frequency noise in MOS transistors—I Theory," *Solid State Electr.*, vol. 11, no. 9, pp. 797-812, Sep. 1968, 10.1016/0038-1101(68)90100-7.
- [2] G. Ghibaudo, O. Roux, Ch. Nguyen-Duc, F. Balestra and J. Brini, "Improved Analysis of Low Frequency Noise in Field-Effect MOS Transistors," *Physica Status Solidi (a)*, vol. 124, no. 2, pp. 571-581, April 1991, 10.1002/pssa.2211240225.
- [3] A. L. McWhorter, "1/f noise and germanium surface properties," *Semiconductor Surface Physics*, pp. 207-228, 1957.
- [4] F. N. Hooge, "1/f noise," *Physica B+C*, vol. 83, no. 1, pp. 14-23, May 1976, 10.1016/0378-4363(76)90089-9.

- [5] C. Enz, and E. Vitoz, "Charge Based MOS Transistor Modeling," Chichester, U. K.:Wiley, 2006, 10.1002/047085546.
- [6] D. M. Binkley, "Tradeoffs and Optimization in Analog CMOS Design," *John Wiley and Sons*, 2008, 10.1002/9780470033715.
- [7] A. C. Ferrari *et al.*, "Science and technology roadmap for graphene, related two-dimensional crystals, and hybrid systems," *Nanoscale*, vol. 7, no. 11, pp. 4598-4810, Sep. 2014, 10.1039/C4NR01600A.
- [8] F. Schwierz, "Graphene transistors," *Nature Nanotechnol.*, vol. 5, no. 7, pp. 487-496, Jul. 2010, 10.1038/nnano.2010.89.
- [9] E. Guerriero, L. Polloni, M. Bianchi, A. Behnam, E. Carrion, L. G. Rizzi, E. Pop and R. Sordan, "Gigahertz Integrated Graphene Ring Oscillators," *ACS Nano*, vol. 7, no. 6, pp. 5588-5594, Jun. 2013, 10.1021/nn401933v.
- [10] S. Castilla, B. Terres, M. Autore, L. Viti, J. Li, A. Y. Nikitin, I. Vangelidis, K. Watanabe, T. Taniguchi, E. Lidorikis, M. S. Vitiello, R. Hillenbrand, K. J. Tielrooij and F. H. L. Koppens, "Fast and Sensitive Terahertz Detection Using an Antenna-Integrated Graphene pn Junction," *Nano Letters*, vol. 19, no. 5, pp. 2765-2773, May 2019, 10.1021/acs.nanolett.8b04171.
- [11] I. Heller, S. Chatoor, J. Mannik, M. A. G. Zevenbergen, J. B. Oostinga, A. F. Morpurgo, C. Dekker and S. G. Lemay, "Charge Noise in Graphene Transistors," *Nano Letters*, vol. 10, no. 5, pp. 1563-1567, May. 2010, 10.1021/nl903665g.
- [12] A. N. Pal, S. Ghatak, V. Kochat, E. S. Sneha, A. Sampathkumar, S. Raghavan and A. Ghosh, "Microscopic Mechanism of 1/f Noise in Graphene: Role of Energy Band Dispersion," *ACS Nano*, vol. 5, no. 3, pp. 2075-2081, March 2011, 10.1021/nn103273n.
- [13] A. A. Balandin, "Low-frequency 1/f noise in graphene devices," *Nature Nanotechnol.*, vol. 8, no. 8, pp. 549-555, Aug. 2013, 10.1038/nnano.2013.144.
- [14] N. Mavredakis, W. Wei, E. Pallecchi, D. Vignaud, H. Happy, R. Garcia Cortadella, A. Bonaccini Calia, J. A. Garrido and D. Jimenez, "Velocity Saturation effect on Low Frequency Noise in short channel Single Layer Graphene FETs," *ACS Applied Electronic Materials*, vol. 1, no. 12, pp. 2626-2636, Dec. 2019, 10.1021/acsaem.9b00604.
- [15] N. Mavredakis, W. Wei, E. Pallecchi, D. Vignaud, H. Happy, R. Garcia Cortadella, N. Schaefer, A. Bonaccini Calia, J. A. Garrido and D. Jimenez, "Low-frequency noise parameter extraction method for single layer graphene FETs," *IEEE Trans. Electron Devices*, vol. 67, no. 5, pp. 93-99, Mar. 2020, 10.1109/TED.2020.2978215.
- [16] D. Jimenez, and O. Moldovan, "Explicit Drain-Current Model of Graphene Field-Effect Transistors Targeting Analog and Radio-Frequency Applications," *IEEE Trans. Electron Devices*, vol. 58, no. 11, pp. 4377-4383, Nov. 2011, 10.1109/TED.2011.2163517.
- [17] W. Wei, X. Zhou, G. Deokar, H. Kim, M. M. Belhaz, E. Galopin, E. Pallecchi, D. Vignaud and H. Happy, "Graphene FETs with Aluminum Bottom-Gate Electrodes and Its Natural Oxide as Dielectrics," *IEEE Trans. Electron Devices*, vol. 62, no. 9, pp. 2769-2773, Sept. 2015, 10.1109/TED.2015.2459657.